Hole Selective Layer Surface Modification and Perovskite Surface Passivation for Efficient Perovskite-Organic Tandem Solar Cells with Record Fill Factor

Md Arafat Mahmud[1,2], Jianghui Zheng[1,2,3,4], Md Habibur Rahman[3], Chwenhaw Liao[1,2], Guoliang Wang[1,2], Shi Tang[1,2], Jueming Bing[1,2], Zhuofeng Li[5], Limei Yang[6,7], Tik Lun Leung[1,2], Hongjun Chen[1,2], Jianpeng Yi[1,2], Stephen P. Bremner[3], Julie Cairney[6], Ashraf Uddin[3], Hieu T. Nguyen[5], and Anita W. Y. Ho-Baillie[1,2,3]**

Affiliations

[1]School of Physics, The University of Sydney, Sydney, NSW 2006, Australia
[2]The University of Sydney Nano Institute (Sydney Nano), The University of Sydney, Sydney, NSW 2006, Australia
[3]Australian Centre for Advanced Photovoltaics (ACAP), School of Photovoltaic and Renewable Energy Engineering, University of New South Wales, Sydney 2052, Australia
[4]Sustainable Energy Research Centre, School of Engineering, Macquarie University, Sydney, NSW 2109, Australia
[5]School of Engineering, The Australian National University, ACT 2601, Australia
[6]Australian Centre for Microscopy and Microanalysis (ACMM), The University of Sydney, Sydney, NSW 2006, Australia
[7]School of Civil and Environmental Engineering, University of Technology Sydney, 81 Broadway, Ultimo, NSW 2007, Australia
*Correspondence to: anita.ho-baillie@sydney.edu.au (A. H.-B.), md.mahmud@sydney.edu.au (M. A. M.)

Metal-halide perovskite based solar cells are the most rapidly advancing photovoltaic technology in terms of efficiency improvement. In 2023, the highest laboratory cell efficiency reached 26.1%,[1] a significant leap from the initial 3.8% reported in 2009[2]. Perovskite solar cells offer several advantages, including tunable bandgaps, which can be maximized in tandem solar cell configurations. Perovskite based double-junction tandem cells have efficiency potential up to 45%[3]. While peovskite-Si tandems have been extensively demonstrated[3], their rigid Si bottom cells pose challenges for flexible applications. Perovskite-CIGS (CIGS: copper indium gallium selenide) tandems are suitable for flexible applications, but the irregularly rough surface of the CIGS bottom cell complicates perovskite top cell fabrication[3]. Additionally, perovskite-perovskite tandems face instability issues due to the tendency for Sn^{2+} to oxidise into Sn^{4+} in low bandgap Sn-Pb based perovskite bottom cell[4].

In contrast, organic photovoltaics (OPV) are a mature, solution-processable technology[5] with significant efficiency improvements in recent years from 11.2% in 2016 to 19.2% in 2023[1]. OPV offers tunable energy levels and bandgaps, making it suitable for tandem applications. Furthermore, low bandgap non-fullerene OPV cells are more stable than low bandgap (1.25 eV) Sn-Pb perovskites, with a projected lifetime of 22 years[6]. Therefore, it is advantageous to combine low bandgap OPV (1.3 eV) with high bandgap (>1.7 eV) perovskite for high-efficiency perovskite-OPV tandems. However, there have been limited demonstrations of perovskite-OPV tandems so far[7].

To realize the full efficiency potential perovskite-OPV tandems, it is necessary to further increase the efficiency of high bandgap perovskite solar cells. Recent advancements in perovskite solar cells have been achieved using self-assembled monolayer (SAM) hole selective layers (HSLs) in perovskite-tandems[7g, 8], leading to impressive power conversion efficiencies. SAM HSLs offer various benefits, including improved morphology and crystallinity of the perovskite layer, enhanced charge selectivity and transport, improved conductivity, and reduced interface recombination. They are also cost-effective due to their ultrathin nature (<5 nm) compared to conventional HSLs (~10-20 nm).

To further enhance the performance of high bandgap perovskite cells using SAM HSLs, reducing the energetic barrier and introducing surface passivation at the perovskite-SAM interface is a

promising strategy. From the design principles, it is also essential for the additional surface passivation layer to lower the highest occupied molecular orbital (HOMO) level of the SAM HSL so that it aligns more closely with the valence band (VB) level of the perovskite. Polycyclic aromatic hydrocarbon (PAH) passivation layers hold significant promise in this context. PAHs, due to their substantial size, can accommodate a substantial separation between positive and negative charges within themselves, resulting in a high dipole moment[9]. This can lead to a potential energy shift or change in work function of the SAM HSL, which is directly proportional to its dipole moment[10]. Therefore, a PAH compound with a substantial positive dipole moment can effectively lower the Fermi level[8a] of the SAM (making it more p-type), thus facilitating hole extraction from the perovskite layer.

Table 1 Demonstrated perovskite-OPV tandems

Perovskite-OPV Tandem				Perovskite Cell				OPV Cell				Ref.
V_{OC} (V)	J_{SC} (mA /cm^2)	FF (%)	PCE (%)	V_{OC} (V)	J_{SC} (mA /cm^2)	FF (%)	PCE (%)	V_{OC} (V)	J_{SC} (mA /cm^2)	FF (%)	PCE (%)	
1.5	10.1	67.0	10.2	0.9	14.1	70.0	9.1	0.7	14.7	68.0	6.6	[7c]
1.6	13.1	75.1	16.0	1.0	15.6	70.6	11.4	Not reported				[11]
1.9	13.1	83.1	20.6	1.1	16.1	83.1	14.7	0.8	25.1	77.0	16.3	[7a]
2.0	12.5	75.6	18.4	1.3	13.5	84.8	14.5	0.8	25.7	71.8	14.4	[7b]
1.9	11.5	71.0	15.1	1.2	16.0	76.0	14.9	0.8	23.4	69.6	12.5	[12]
2.0	13.3	80.8	21.1	1.2	15.8	81.6	15.5	0.8	26.1	74.0	16.0	[7f]
2.1	14.8	77.2	23.6	1.3	17.9	78.9	17.8	0.8	26.8	74.8	16.8	[7i]
1.9	12.6	79.0	19.2	1.1	16.2	80.0	14.0	0.9	25.2	72.0	15.6	[7j]
2.2	14.0	80.0	24.0	1.3	15.6	81.0	16.8	0.9	26.7	75.0	17.5	[7g]
1.9	13.8	70.5	18.0	1.2	18.1	67.1	14.3	0.7	24.9	62.8	11.1	[8c]
2.0	**12.8**	**83.6**	**21.5**	**1.3**	**17.5**	**82.7**	**18.0**	**0.8**	**26.5**	**70.2**	**15.4**	**This work**

In this work, we have applied a novel halogenated PAH compound onto the SAM-HSL in perovskite cells. More details of the compound and cell fabrication processes will be presented in the conference. It was found that PAH induces a high surface dipole[14] at the perovskite-SAM interface, and reduces the energetic barrier for hole extraction by 210 meV compared to cells with non-treated SAM by downshifting the HOMO level of PAH-SAM-HSL closer to the perovskite VBM. This modification also slightly blue-shifted the perovskite bandgap due to the partial diffusion of halide anions from halogenated PAH layer into the perovskite film providing bulk and interface passivation. The resulting single-junction high bandgap inverted devices showed significant improvements in voltage output and fill factor (FF), achieving a champion efficiency of 18%. The efficiency is the highest among the high bandgap cells used for perovskite-OPV tandem cells (Fig. 1a and Table 1). Also, the FF achieved (82.7%) is the highest among the SAM-HSL-based-high-bandgap-perovskite-cells for perovskite-OPV tandem (Fig. 1b), due to a low band-offset between perovskite VBM and HSL HOMO (Fig. 1f).

When incorporated into a perovskite-OPV tandem cell, the halogenated PAH treatment of HSL led to a champion power conversion efficiency of 21.5% and an outstanding fill factor of 83.6%. This is the highest fill factor reported in peer-reviewed reports of perovskite-OPV tandem solar cells (Table 1) and paves the way for further developments in functionalized PAH compounds for high-efficiency perovskite and perovskite-based tandem solar cells.

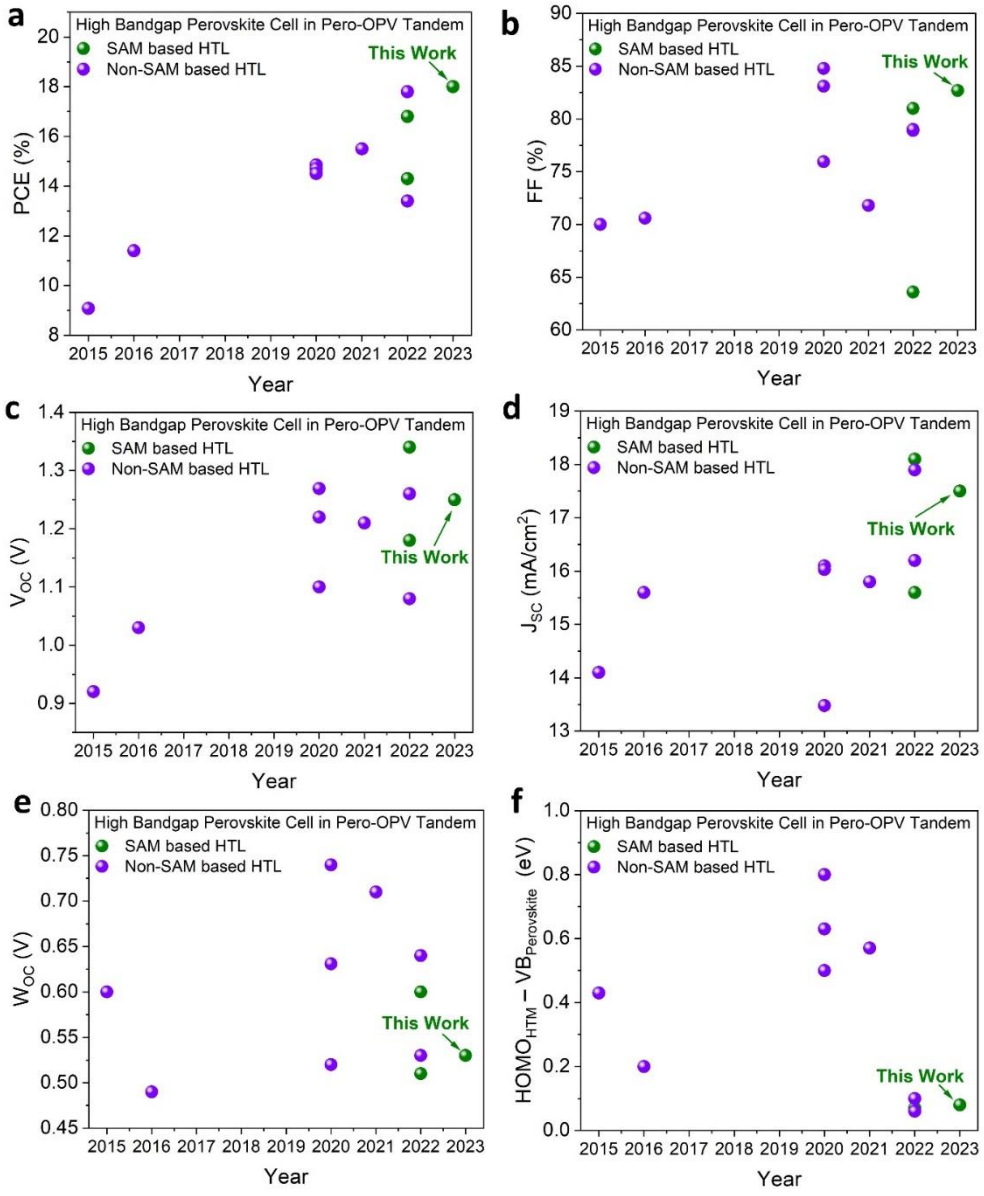

Figure 1. a. PCE, b. FF, c. V_{OC}, d. J_{SC} and e. W_{OC} and f. $HOMO_{HTM} - VB_{perovskite}$ evolution for high bandgap perovskite in this work and in previously reported perovskite-OPV tandems [7a-h, 13].

References

[1] NREL Best Research Cell Efficiency Chart, https://www.nrel.gov/pv/cell-efficiency.html, accessed: 1 October, 2021.

[2] M. A. Green, A. Ho-Baillie, H. J. Snaith, *Nature Photonics* **2014**, 8, 506.

[3] A. W. Y. Ho-Baillie, J. Zheng, M. A. Mahmud, F.-J. Ma, D. R. McKenzie, M. A. Green, **2021**, 8, 041307.

[4] R. Lin, K. Xiao, Z. Qin, Q. Han, C. Zhang, M. Wei, M. I. Saidaminov, Y. Gao, J. Xu, M. Xiao, A. Li, J. Zhu, E. H. Sargent, H. Tan, *Nature Energy* **2019**, DOI: 10.1038/s41560-019-0466-3.

[5] M. B. Upama, M. A. Mahmud, G. Conibeer, A. Uddin, *Solar RRL* **2020**, 4, 1900342.

[6] X. Xu, J. Xiao, G. Zhang, L. Wei, X. Jiao, H.-L. Yip, Y. Cao, *Science Bulletin* **2020**, 65, 208.

[7] a) X. Chen, Z. Jia, Z. Chen, T. Jiang, L. Bai, F. Tao, J. Chen, X. Chen, T. Liu, X. Xu, C. Yang, W. Shen, W. E. I. Sha, H. Zhu, Y. Yang, *Joule* **2020**, 4, 1594; b) S. Xie, R. Xia, Z. Chen, J. Tian, L. Yan, M. Ren, Z. Li, G. Zhang, Q. Xue, H.-L. Yip, Y. Cao, *Nano Energy* **2020**, 78, 105238; c) C.-C. Chen, S.-H. Bae, W.-H. Chang, Z. Hong, G. Li, Q. Chen, H. Zhou, Y. Yang, *Materials Horizons* **2015**, 2, 203; d) Y. Liu, L. A. Renna, M. Bag, Z. A. Page, P. Kim, J. Choi, T. Emrick, D. Venkataraman, T. P. Russell, *ACS Applied Materials & Interfaces* **2016**, 8, 7070; e) Z. Li, S. Wu, J. Zhang, K. C. Lee, H. Lei, F. Lin, Z. Wang, Z. Zhu, A. K. Y. Jen, **2020**, 10, 2000361; f) P. Wang, W. Li, O. J. Sandberg, C. Guo, R. Sun, H. Wang, D. Li, H. Zhang, S. Cheng, D. Liu, J. Min, A. Armin, T. Wang, *Nano Letters* **2021**, 21, 7845; g) K. O. Brinkmann, T. Becker, F. Zimmermann, C. Kreusel, T. Gahlmann, M. Theisen, T. Haeger, S. Olthof, C. Tückmantel, M. Günster, T. Maschwitz, F. Göbelsmann, C. Koch, D. Hertel, P. Caprioglio, F. Peña-Camargo, L. Perdigón-Toro, A. Al-Ashouri, L. Merten, A. Hinderhofer, L. Gomell, S. Zhang, F. Schreiber, S. Albrecht, K. Meerholz, D. Neher, M. Stolterfoht, T. Riedl, *Nature* **2022**, 604, 280; h) H. Xu, L. Torres Merino, M. Koc, E. Aydin, S. Zhumagali, M. A. Haque, A. Yazmaciyan, A. Sharma, D. Rosas Villalva, L. Huerta Hernandez, M. De Bastiani, M. Babics, F. H. Isikgor, J. Troughton, S. De Wolf, S. Yerci, D. Baran, *ACS Applied Energy Materials* **2022**, DOI: 10.1021/acsaem.2c01749; i) W. Chen, Y. Zhu, J. Xiu, G. Chen, H. Liang, S. Liu, H. Xue, E. Birgersson, J. W. Ho, X. Qin, J. Lin, R. Ma, T. Liu, Y. He, A. M.-C. Ng, X. Guo, Z. He, H. Yan, A. B. Djurišić, Y. Hou, *Nature Energy* **2022**, 7, 229; j) Z. Zhang, C. Cueto, Y. Ding, L. Yu, T. P. Russell, T. Emrick, Y. Liu, *ACS Applied Materials & Interfaces* **2022**, 14, 29896.

[8] a) A. Al-Ashouri, A. Magomedov, M. Roß, M. Jošt, M. Talaikis, G. Chistiakova, T. Bertram, J. A. Márquez, E. Köhnen, E. Kasparavičius, S. Levcenco, L. Gil-Escrig, C. J. Hages, R. Schlatmann, B. Rech, T. Malinauskas, T. Unold, C. A. Kaufmann, L. Korte, G. Niaura, V. Getautis, S. Albrecht, *Energy & Environmental Science* **2019**, 12, 3356; b) A. Al-Ashouri, E. Köhnen, B. Li, A. Magomedov, H. Hempel, P. Caprioglio, J. A. Márquez, A. B. M. Vilches, E. Kasparavicius, J. A. Smith, *Science* **2020**, 370, 1300; c) H. Xu, L. Torres Merino, M. Koc, E. Aydin, S. Zhumagali, M. A. Haque, A. Yazmaciyan, A. Sharma, D. Rosas Villalva, L. Huerta Hernandez, M. De Bastiani, M. Babics, F. H. Isikgor, J. Troughton, S. De Wolf, S. Yerci, D. Baran, *ACS Applied Energy Materials* **2022**, 5, 14035; d) J. Liu, M. De Bastiani, E. Aydin, G. T. Harrison, Y. Gao, R. R. Pradhan, M. K. Eswaran, M. Mandal, W. Yan, A. Seitkhan, M. Babics, A. S. Subbiah, E. Ugur, F. Xu, L. Xu, M. Wang, A. u. Rehman, A. Razzaq, J. Kang, R. Azmi, A. A. Said, F. H. Isikgor, T. G. Allen, D. Andrienko, U. Schwingenschlögl, F. Laquai, S. De Wolf, **2022**, 377, 302.

[9] Q. Tao, M. Xiao, M. Zhu, L. Shao, Z. Sui, P. Wang, G. Huang, Y. Pei, W. Zhu, F. Huang, *Dyes and Pigments* **2017**, 144, 142.

[10] J. B. Rivest, G. Li, I. D. Sharp, J. B. Neaton, D. J. Milliron, *The Journal of Physical Chemistry Letters* **2014**, 5, 2450.

[11] Y. Liu, L. A. Renna, M. Bag, Z. A. Page, P. Kim, J. Choi, T. Emrick, D. Venkataraman, T. P. Russell, *ACS Appl Mater Interfaces* **2016**, 8, 7070.

[12] Z. Li, S. Wu, J. Zhang, K. C. Lee, H. Lei, F. Lin, Z. Wang, Z. Zhu, A. K. Y. Jen, *Advanced Energy Materials* **2020**, 10, 2000361.

[13] W. Chen, Y. Zhu, J. Xiu, G. Chen, H. Liang, S. Liu, H. Xue, E. Birgersson, J. W. Ho, X. Qin, J. Lin, R. Ma, T. Liu, Y. He, A. M.-C. Ng, X. Guo, Z. He, H. Yan, A. B. Djurišić, Y. Hou, *Nature Energy* **2022**, DOI: 10.1038/s41560-021-00966-8.